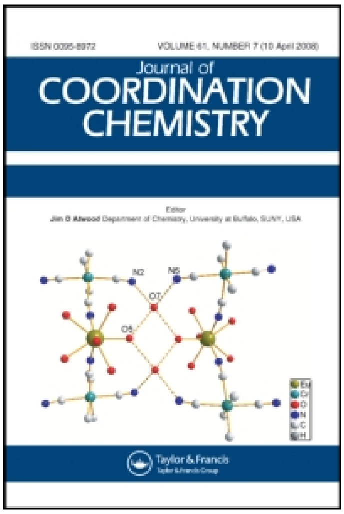

Journal of Coordination Chemistry
Publication details, including instructions for authors and subscription information:
http://www.informaworld.com/smpp/title~content=t713455674

Synthesis, electrochemical and antimicrobial studies of mono and binuclear iron(III) and oxovanadium(IV) complexes of [ONO] donor tridentate Schiff-base ligands

Chira R. Bhattacharjee[a]; Pankaj Goswami[b]; Mahuya Sengupta[c]
[a] Department of Chemistry, Assam University, Silchar 788011, Assam, India [b] Department of Chemistry, Silchar Polytechnic, Silchar 788015, Assam, India [c] Department of Biotechnology, Assam University, Silchar 788011, Assam, India

First published on: 21 October 2010

To cite this Article Bhattacharjee, Chira R. , Goswami, Pankaj and Sengupta, Mahuya(2010) 'Synthesis, electrochemical and antimicrobial studies of mono and binuclear iron(III) and oxovanadium(IV) complexes of [ONO] donor tridentate Schiff-base ligands', Journal of Coordination Chemistry, 63: 22, 3969 — 3980, First published on: 21 October 2010 (iFirst)
To link to this Article: DOI: 10.1080/00958972.2010.525703
URL: http://dx.doi.org/10.1080/00958972.2010.525703

Journal of Coordination Chemistry
Vol. 63, No. 22, 20 November 2010, 3969–3980

Synthesis, electrochemical and antimicrobial studies of mono and binuclear iron(III) and oxovanadium(IV) complexes of [ONO] donor tridentate Schiff-base ligands

CHIRA R. BHATTACHARJEE*†, PANKAJ GOSWAMI‡ and
MAHUYA SENGUPTA§

†Department of Chemistry, Assam University, Silchar 788011, Assam, India
‡Department of Chemistry, Silchar Polytechnic, Silchar 788015, Assam, India
§Department of Biotechnology, Assam University, Silchar 788011, Assam, India

(*Received 20 April 2010; in final form 26 August 2010*)

Tridentate Schiff bases (H_2L^1 or H_2L^2) were derived from condensation of acetylacetone and 2-aminophenol or 2-aminobenzoic acid. Binuclear square pyramidal complexes of the type $[M_2(L^1)_2]\cdot nH_2O$ ($M = Fe–Cl$, $n = 0$; $M = VO$, $n = 1$) were accessed from interaction of H_2L^1 with anhydrous $FeCl_3$ and $VOSO_4\cdot 5H_2O$, respectively. A similar reaction with H_2L^2, however, produced mononuclear complexes $[ML^2(H_2O)_x]\cdot nH_2O$ ($M=Fe–Cl$, $x = 0$, $n = 0$; $M=VO$, $x = 1$, $n = 1$). The compounds were characterized using elemental analysis, FT-IR, UV-Vis, and NMR (for ligand only), and mass spectroscopies and solution electrical conductivity studies. Magnetic susceptibility measurements suggest antiferromagnetic exchange in binuclear Fe(III) and VO(IV) complexes. Thermo gravimetric analysis (TGA) provided unambiguous evidence for the presence of coordinated as well as lattice water in $[VOL^2(H_2O)]\cdot H_2O$. Cyclic voltammetric studies showed well-defined redox processes corresponding to Fe(III)/Fe(II) and VO(V)/VO(IV). *In vitro* antimicrobial activities of the compounds were investigated against *Klebsiella pneumoniae*, *Staphylococcus aureus*, *Pseudomonas aeroginosa*, *Escherichia coli*, *Bacillus subtilis*, and *Proteus vulgaris*. H_2L^1 and its binuclear complexes exhibited pronounced activity against all the microorganisms tested.

Keywords: Schiff bases; Acetylacetone; Oxovanadium(IV) complexes; Iron(III) complexes; Antimicrobial activity

1. Introduction

Metal-Schiff base complexes have synthetic proclivity, structural diversity, and potential application in pharmacology and catalysis [1]. Design, synthesis, and characterization of Schiff bases and complexation with transition metals are focus of current research in coordination chemistry. Dinuclear complexes which serve as models mimicking metallobiosites are of particular interest [2, 3]. Potential applications like separation materials, catalysis precursors, models of the catalyze enzymes [4–7], and interesting structures [8–10] have spurred research in this field. Amino acid based Schiff bases and their first row transition metal complexes were reported to exhibit fungicidal,

---

*Corresponding author. Email: crbhattacharjee@rediffmail.com

Journal of Coordination Chemistry
ISSN 0095-8972 print/ISSN 1029-0389 online © 2010 Taylor & Francis
DOI: 10.1080/00958972.2010.525703

bactericidal, antiviral, and antitubercular activity [11–13]. Use of iron-Schiff base complexes in different catalytic reactions has been reported in recent work [14–16]. Schiff bases derived from 2,4-pentanedione/1-phenyl-1,3-butanedione and ethylenediamine have been reported [17]. The development of β-diketone-based Schiff base and their transition metal complexes as antimicrobial agents is very attractive. Complexes of vanadium(IV/V) with tridentate [ONO] donor Schiff-base ligands have been reviewed [18]. Structural and functional models for vanadium-dependent enzymes have also stimulated the coordination chemistry of the metal [19, 20]; β-diketone-based dibasic tridentate [ONO] donor Schiff-base ligands form vanadium(IV/V) complexes under anaerobic conditions [21–23]. Recently, we reported the synthesis and reactivity of $[Fe(acacen)(H_2O)_2]NO_3$ incorporating a quadridentate Schiff base [24].

Herein, we report the synthesis and structural characterization of Fe(III) and VO(IV) complexes with tridentate [ONO] donor Schiff bases derived from acetylacetone and 2-aminophenol or 2-aminobenzoic acid. Magnetic, thermal, and electrochemical behavior of the complexes are also studied. *In-vitro* antimicrobial activities of these compounds against *Klebsiella pneumoniae*, *Staphylococcus aureus*, *Pseudomonas aeroginosa*, *Escherichia coli*, *Bacillus subtilis*, and *Proteus vulgaris* are also incorporated.

2. Experimental

2.1. *Materials*

Reagent grade and HPLC grade solvents and chemicals were used. Acetylacetone, ethanol, methanol, and other solvents were distilled prior to use. In this study, 2-aminophenol and 2-aminobenzoic acid were obtained from Qualigens Fine Chemicals and recrystallized before use. Anhydrous ferric chloride and vanadyl sulfate pentahydrate were obtained from E. Merck India Ltd. and used as received.

2.2. *Measurements*

Microanalytical (C, H, and N) data were obtained with a Perkin Elmer Model 240C elemental analyzer. Infrared spectra were obtained using KBr pellets on a Spectrum BX series FT-IR spectrophotometer from 400–4000 cm^{-1}. Electronic spectra were recorded in DCM on a Shimadzu 1600-PC UV-Vis spectrophotometer from 200 to 800 nm. Nuclear magnetic resonance spectra (^1H and ^{13}C) were acquired from a Bruker Advance 300 MHz FT-NMR Spectrometer using $CDCl_3$ as solvent and TMS as internal standard. Mass spectra were recorded on a Jeol SX-102 spectrometer with fast atom bombardment. Molar conductances of the complexes were determined in DMSO (*ca* 10^{-3} mol L^{-1}) at room temperature using a Toa CM 405 conductivity meter. Magnetic susceptibilities of the complexes were measured at room temperature on a Lakeshore 7407 Vibrating Sample Magnetometer from –20,000 to 20,000 gauss. Thermal investigation of the sample was recorded on a PYRIS DIAMOND thermal analyzer under dynamic flow of nitrogen (100 mL min^{-1}) and heating rate of 10°C min^{-1} from ambient temperature to 1000°C. The number of decomposition steps was identified with DTG. Electrochemical behaviors of the complexes were investigated by cyclic voltammetry in a CHI 660C Electrochemical Workstation in dicholoromethane *versus* SCE at room temperature in the potential range −1.0 to 1.0 V. Antimicrobial activities of the compounds were evaluated by Kirby–Bauer disc diffusion method using ethanol as solvent as well as control and tetracycline as standard drug.

3. Synthesis

3.1. *Schiff base (H_2L^1)*

The ligand was prepared from condensation of acetylacetone and 2-aminophenol in 1 : 1 molar ratio. Also, 2-aminophenol (10 mmol, 1.09 g) was dissolved in dry ethanol and then added to an ethanolic solution of acetylacetone (10 mmol, 1.00 g) containing a few drops of acetic acid and the mixture was refluxed for 4 h. The solvent was then removed on a rotary evaporator and the residue crystallized at room temperature. The yellow crystals so obtained were recrystallized from methanol. Yield 69% and melting point 188°C. Elemental Anal. (%) Calcd C (69.11), H (6.81), and N (7.32). Found C (68.92), H (6.84), and N (7.55). FT-IR (KBr pellets, ν cm^{-1}) 1166 (C–O), 1351 (C–O), 1614 (C=N), and 3451 (O–H). UV-Vis (CH_2Cl_2, λ_{max} nm, ε (mol L^{-1})$^{-1}$ cm^{-1}) 235 (11,460), and 312 (32,320). ^{1}H-NMR (300 MHz, δ ppm, from TMS in $CDCl_3$) 11.72 (s, 1H, OH), 9.01 (s, 1H, OH), 6.82–7.19 (m, 4H, ring proton), 5.17 (s, 1H, –CH=C<), 2.06 (s, 3H, CH_3), and 1.84 (s, 3H, CH_3). ^{13}C-NMR (300 MHz, δ ppm, from TMS in $CDCl_3$) 19.61, 28.61, 97.35, 117.26, 120.13, 125.37, 128.00, 128.74, 152.44, 163.46, and 196.23. MS (m/z) 191.9[M]$^+$, 173.9, and 133.8.

3.2. *Schiff base (H_2L^2)*

The ligand was prepared by a procedure similar to that of H_2L^1 using 2-aminobenzoic acid (10 mmol, 1.37 g) instead of 2-aminophenol. Yield 66% and melting point 148°C. Elemental Anal. (%) Calcd C (65.75), H (5.93), and N (6.39). Found C (65.94), H (5.74), and N (6.55). FT-IR (KBr pellets, ν cm^{-1}) 1166 (C–O), 1215 (C–O), 1599 (C=N), and 3414 (O–H). UV-Vis (CH_2Cl_2, λ_{max} nm, ε (mol L^{-1})$^{-1}$ cm^{-1}) 247 (20,060), and 341 (15,300). ^{1}H-NMR (300 MHz, δ ppm, from TMS in $CDCl_3$) 12.97 (s, 1H, OH), 6.63–8.04 (m, 4H, ring proton), 5.26 (s, 1H, –CH=C<), 1.67 (s, 3H, CH_3), and 1.25 (s, 3H, CH_3). ^{13}C-NMR (300 MHz, δ ppm, from TMS in $CDCl_3$) 20.54, 24.86, 99.95, 116.38, 124.60, 125.27, 132.09, 135.80, 151.04, 162.82, 168.50, and 196.65. MS (m/z) 219.9[M]$^+$, 201.9, and 161.8.

3.3. *Synthesis of iron(III) complex, [$Fe_2(L^1)_2Cl_2$]*

H_2L^1 (1 mmol, 0.191 g) dissolved in ethanol (20 cm^3) was added to an ethanol solution (20 cm^3) of anhydrous $FeCl_3$ (1 mmol, 0.162 g) and the mixture was refluxed for 3 h. On standing overnight, pale brown complex precipitated was filtered off, washed with cold ethanol, recrystallized from methanol, and dried in air. Yield 58% and melting point >300°C. Elemental Anal. (%) Calcd C (47.05), H (3.92), and N (4.99). Found C (47.31), H (3.88), and N (5.16). FT-IR (KBr pellets, ν cm^{-1}) 443 (Fe–O), 546 (Fe–N), 1218 (C–O), 1315 (C–O), and 1604 (C=N). UV-Vis (CH_2Cl_2, λ_{max} nm, ε $(mol\,L^{-1})^{-1}\,cm^{-1}$) 250 (28,200), 315 (17,530), 364 (20,340), 441 (16,550), 462 (16,210), and 717 (440). MS (FAB, *m*/*z*) 561$[M]^+$, 489, and 281.

3.4. *Synthesis of oxovanadium(IV) complex, $[(VO)_2(L^1)_2]\cdot H_2O$*

The complex was prepared by a procedure similar to that of $[Fe_2(L^1)_2Cl_2]$ with $VOSO_4 \cdot 5H_2O$ (1 mmol, 0.253 g) instead of anhydrous $FeCl_3$. The green complex was obtained in 63% yield with melting point >300°C. Elemental Anal. (%) Calcd C (49.81), H (4.52), and N (5.28). Found C (49.63), H (4.78), and N (5.06). FT-IR (KBr pellets, ν cm^{-1}) 460 (V–O), 530 (V–N), 966 (V=O), 1212 (C–O), 1319 (C–O), 1596 (C=N), and 3403 (O–H). UV-Vis (CH_2Cl_2, λ_{max} nm, ε $(mol\,L^{-1})^{-1}\,cm^{-1}$) 231 (18,500), and 410 (7250). MS (FAB, *m*/*z*) 529$[M]^+$, 512, and 254.

3.5. *Synthesis of iron(III) complex, $[Fe(L^2)Cl]$*

The complex was prepared by a procedure similar to that of $[Fe_2(L^1)_2Cl_2]$ using H_2L^2 (1 mmol, 0.219 g) instead of H_2L^1. Yield 61% of brown product with melting point 122°C. Elemental Anal. (%) Calcd C (46.67), H (3.56), and N (4.53). Found C (46.93), H (3.68), and N (4.36). FT-IR (KBr pellets, ν cm^{-1}) 483 (Fe–O), 528 (Fe–N), 1255 (C–O), 1301 (C–O), and 1578 (C=N). UV-Vis (CH_2Cl_2, λ_{max} nm, ε $(mol\,L^{-1})^{-1}\,cm^{-1}$) 230 (20,650), 250 (28,200), 247 (18,250), 334 (10,000), and 493 (250). MS (FAB, *m*/*z*) 309$[M]^+$.

3.6. *Synthesis of $[VO(L^2)(H_2O)]\cdot H_2O$*

The complex was prepared by a procedure similar to that of $[(VO)_2(L^1)_2]\cdot H_2O$ using H_2L^2 (1 mmol, 0.219 g) instead of H_2L^1. Yield 56% of pale green product decomposing at 140°C. Elemental Anal. (%) Calcd C (45.00), H (4.68), and N (4.37). Found C (45.36), H (4.48), and N (4.53). FT-IR (KBr pellets, ν cm^{-1}) 488 (V–O), 539 (V–N), 656 ($\rho_{wagg}H_2O$), 906 ($\rho_{rock}H_2O$), 976 (V=O), 1242 (C–O), 1303 (C–O), 1586 (C=N), and 3364 (O–H). UV-Vis (CH_2Cl_2, λ_{max} nm, ε $(mol\,L^{-1})^{-1}\,cm^{-1}$) 254 (29,400), 276 (28,400), 299 (35,400), and 493 (200). MS (FAB, *m*/*z*) 320$[M]^+$ and 284.

4. Results and discussion

4.1. *Chemistry*

A condensation reaction occurred between acetylacetone and 2-aminophenol or 2-aminobenzoic acid in 1 : 1 molar ratio yielding yellow H_2L^1 or H_2L^2 in weakly acidic medium (scheme 1). Acetylacetone mostly exists in enol form at room temperature and under mild acidic conditions offers only one carbonyl for condensation with amines. This reactivity trend is typical of β-diketone chemistry. Formation of Schiff bases was confirmed by FT-IR, UV-Vis, ^1H–NMR, and ^{13}C-NMR, and mass spectroscopies. Iron(III) and oxovanadium(IV) complexes were prepared in good yield

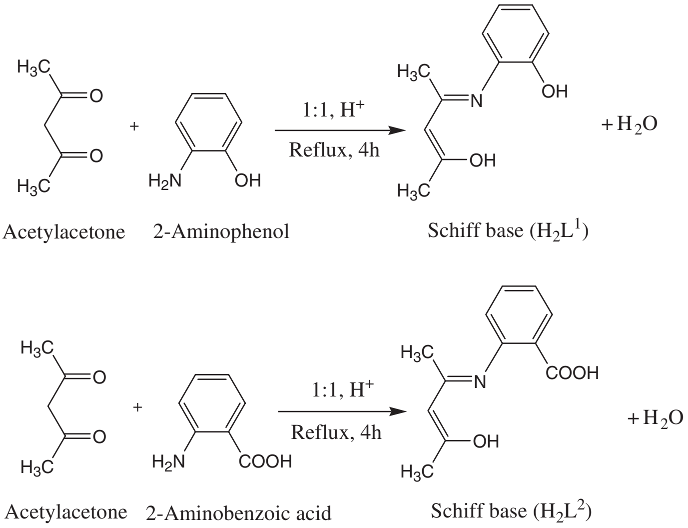

Scheme 1. Synthesis of Schiff bases.

by reaction of the Schiff-base ligands with anhydrous ferric chloride or vanadyl sulfate pentahydrate in 1 : 1 molar ratio (scheme 2).

The compounds are soluble in polar solvents (ethanol, methanol, chloroform, dichloromethane, and dimethylsulfoxide) but insoluble in non-polar solvents. Based on physical studies, a distorted square pyramidal binuclear structure involving two tridentate [ONO] donors with the phenoxide group of each ligand bridging the metal centers has been proposed for complexes with H_2L^1. Five-coordinate square pyramidal dimeric copper(II) and vanadyl(IV) complexes of H_2L^1 have been reported [25]. [NO_2] donor Schiff base derived from 2-hydroxy-5-methylacetophenone and glycine and its complexes with a number of divalent metal ions including Fe(II) [26] and mononuclear ion-pair complexes of Co(II) and Fe(II) with [NO_2] donor salicylidenglycine Schiff base have recently been reported [27]. However, a distorted mononuclear structure with Cl^- occupying the fourth site in Fe(III) complex and a square pyramidal structure with aquo occupying the fifth site for VO(IV) have been proposed for complexes with H_2L^2. Formation of both dinuclear and mononuclear complexes with dibasic tridentate [ONO] Schiff-base ligands can be attributed to the difference in the stereochemical disposition of OH in the aromatic ring. This aspect can be exploited further to access newer mono or dinuclear complexes.

4.2. *IR spectra*

The free ligands show stretching modes attributed to C=N, C–O, and O–H in the range 1599–1614, 1166–1351, and 3414–3451 cm^{-1}, respectively. On complexation, the C=N band shifted to lower wavenumber, indicating coordination through the azomethine nitrogen to the metal [28]. Bands due to ν(O–H) were absent in the complexes, indicating coordination through deprotonated ligand. Coordination of oxygen and azomethine nitrogen in the complexes is further supported by the appearance of

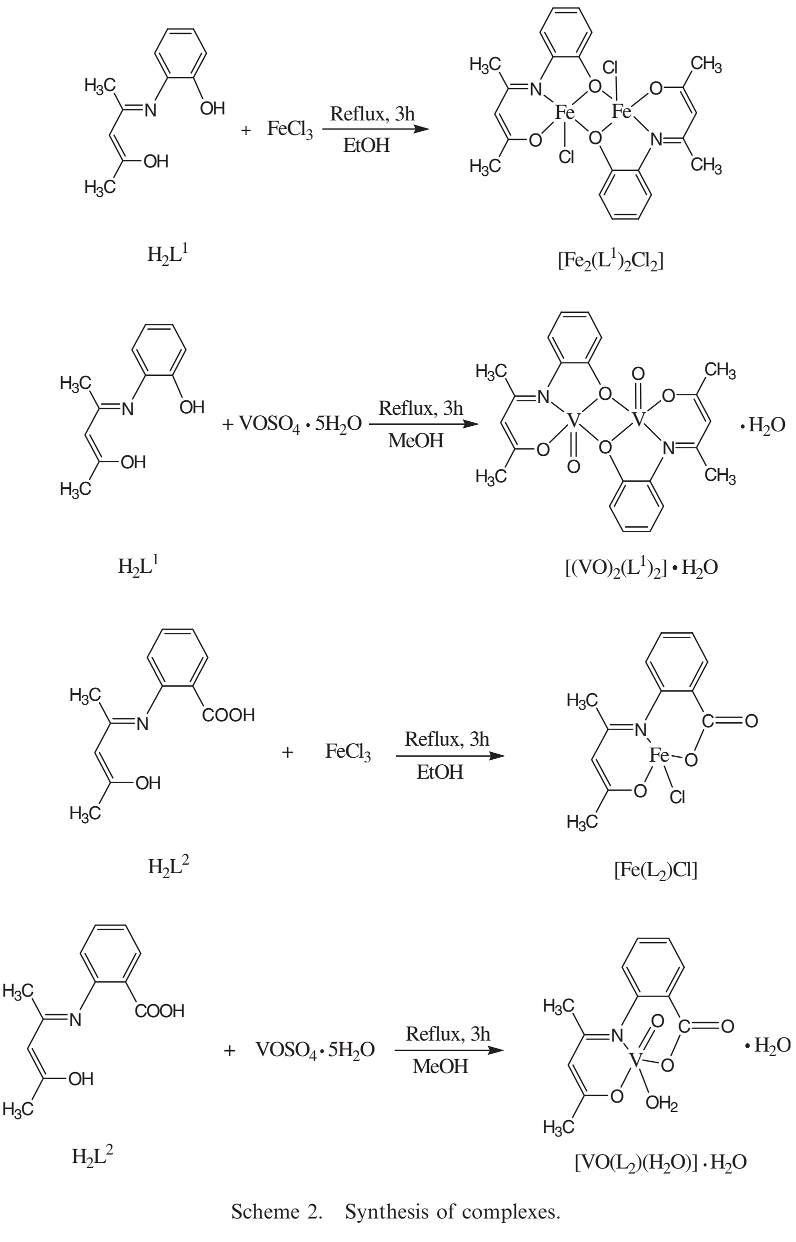

Scheme 2. Synthesis of complexes.

ν(M–O) and ν(M–N) in the range 443–488 and 528–546 cm^{-1}, respectively [29]. The oxovanadium(IV) complexes showed a strong band at *ca* 970 cm^{-1} attributed to stretching of the vanadyl (V=O) with linear chain $V{=}O \cdots V{=}O$ interaction being absent [30]. Spectra of both mono and dinuclear oxovanadium(IV) complexes show OH mode from lattice water. Additional bands at 906 and at 656 cm^{-1} in the mononuclear oxovanadium(IV) complex attributable to rocking and wagging modes of coordinated water attest to the presence of water [31].

4.3. *Electronic spectra*

Electronic spectra of the ligands and complexes in dichloromethane exhibited high intensity bands at 235–341 nm attributed to intraligand $\pi \rightarrow \pi^*$ and $n \rightarrow \pi^*$ transitions [32]. Lower energy bands (364–462 nm) in complexes are due to ligand-to-metal charge transfer (LMCT) transition [33, 34]. Low intensity bands at 717 nm ($\varepsilon = 440$ $(\text{mol L}^{-1})^{-1}\text{cm}^{-1}$) in binuclear Fe(III) complex and at 493 nm ($\varepsilon = 250$ $(\text{mol L}^{-1})^{-1}\text{cm}^{-1}$) in mononuclear Fe(III) complex arises from partly allowed $^6A_1 \rightarrow$ excited state d–d transitions, confirming high spin iron(III) [35]. A very weak band at *ca* 490 nm ($\varepsilon = 200$ $(\text{mol L}^{-1})^{-1}\text{cm}^{-1}$) in the mononuclear vanadyl complex is presumably due to $^2B_2 \rightarrow {}^2E$ transition [35].

4.4. *NMR spectra*

^{1}H-NMR spectra of H_2L^1 and H_2L^2 revealed a singlet at 11.72 and 12.97 ppm, respectively, for the proton of the hydroxyl. Multiplets in the range 6.63–8.04 ppm are attributable to protons of benzene. Sharp singlets at 5.17, 2.06, and 1.84 ppm in H_2L^1 and 5.26, 1.67, and 1.25 ppm in H_2L^2 are due to olefinic proton (–CH=C<) and magnetically non-equivalent methyl protons (–CH_3), respectively.

The ^{13}C-NMR spectra of the ligands showed resonances concordant with magnetically non-equivalent carbons. The azomethine carbon is at 163 ppm in both ligands. Resonances at 19.61–28.61 ppm are due to carbons of the magnetically non-equivalent methyls. Carbons of benzene showed resonances from 116 to 152 ppm; –CH= is at 97.35 and 99.95 ppm in H_2L^1 and H_2L^2, respectively. Resonances around 196 ppm in both ligands are due to the carbon of =C–OH group, while carbon of –COOH group of H_2L^2 was at 168.50 ppm.

4.5. *Mass spectra*

Mass spectra of the compounds were recorded in FAB$^+$ ionization mode. The molecular ion peak of H_2L^1 and H_2L^2 appeared at *m*/*z* 191 and 219, respectively, along with other assignable fragments. The molecular formula $Fe_2C_{22}H_{22}N_2O_4Cl_2$, $V_2C_{22}H_{24}N_2O_7$, $FeC_{12}H_{11}NO_3Cl$, and $VC_{12}H_{15}NO_6$ suggested for the complexes were confirmed by observed peak at *m*/*z* 561 (*ca* 561), 529 (*ca* 530), 309 (*ca* 308.5), and 320 (*ca* 320), respectively. The peak at *m*/*z* 284 observed for the complex $[VO(L^2)(H_2O)] \cdot H_2O$ is attributed to $[M - 2H_2O]^+$ species arising from the loss of coordinated as well as lattice water. In addition to $[M]^+$ peak, the binuclear complex of Fe(III) showed appearance of $[M+2]^+$ as well as $[M+4]^+$ peak. In mononuclear Fe(III) complex, $[M+2]^+$ was observed along with molecular ion peak. The isotopic peak was observed further in all the fragments containing chlorine. The probable fragmentation patterns of the ligands and binuclear Fe(III) and VO(IV) complexes are provided in "Supplementary material" (schemes 1S and 2S).

4.6. *Molar conductance*

Molar conductances of $[Fe_2(L^1)_2Cl_2]$, $[(VO)_2(L^1)_2] \cdot H_2O$, $[Fe(L^2)Cl]$, and $[VO(L^2)(H_2O)] \cdot H_2O$ in DMSO (*ca* 10^{-3}mol L^{-1}) were found to be 13.1, 9.2, 11.6, and 9.8 $\Omega^{-1}\text{cm}^2\text{mol}^{-1}$, respectively, suggesting non-electrolytes [36].

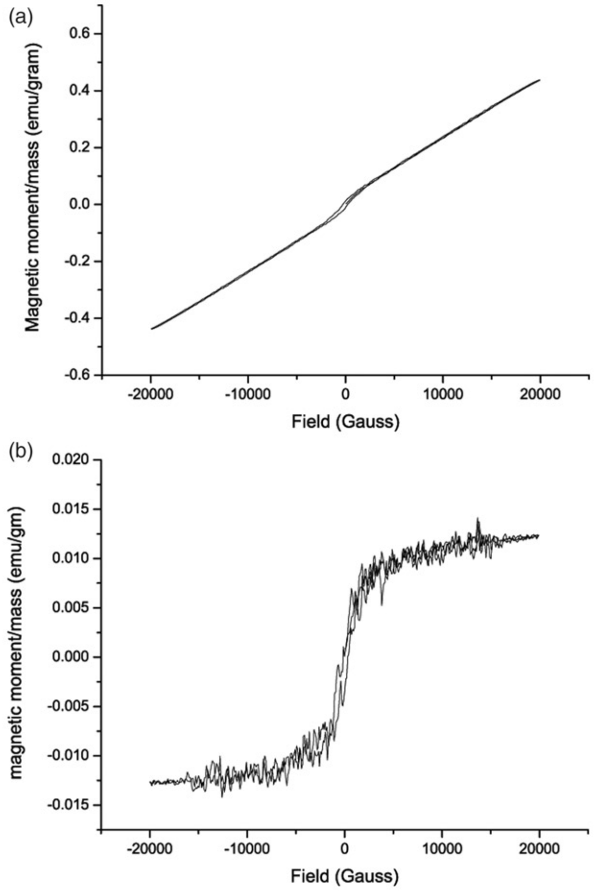

Figure 1. Field dependence of magnetization of (a) $[Fe_2(L^1)_2Cl_2]$ and (b) $[VO(L^2)(H_2O)] \cdot H_2O$.

4.7. *Magnetic susceptibility*

Room temperature magnetic susceptibilities of $[Fe_2(L^1)_2Cl_2]$ and $[(VO)_2(L^1)_2] \cdot H_2O$ were conducted using a Vibrating Sample Magnetometer. The magnetizations *versus* magnetic field (figure 1) were examined from –20,000 to 20,000 gauss. The parameters extracted from the hysteresis loop are the saturation magnetization (Ms), the remanence (Mr), the coercivity (Hc), the squareness ratio (SQR), and the initial slope (table 1).

The effective magnetic moments of the complexes are then calculated from the initial slope of the hysteresis using the relation

$$\mu_{\mathrm{eff}} = 2.827 \times \oplus\left(\chi'_{\mathrm{M}} \times \mathrm{T}\right),\ \chi'_{\mathrm{M}} = \chi_{\mathrm{M}} - \chi_{\mathrm{dia}}$$

where χ_{dia} is diamagnetic correction. The diamagnetic corrections are calculated by summing the contributions from the atoms, ions, and bonds of the molecule. These group contributions are known as Pascal's constants.

The magnetic moment values of $[Fe_2(L^1)_2Cl_2]$ and $[(VO)_2(L^1)_2] \cdot H_2O$ at room temperature were 5.36 and 1.13 B.M., respectively, supporting a high spin, strongly

Table 1. Magnetic behavior of the complexes.

Compounds	Ms ($\times 10^{-3}$)	Mr ($\times 10^{-3}$)	Hc	SQR	Initial slope ($\times 10^{-6}$)	μ_{eff} (B.M.)
$[Fe_2(L^1)_2Cl_2]$	434.851	11.552	238.51	0.02656	19.167	5.36
$[(VO)_2(L^1)_2] \cdot H_2O$	14.186	1.828	245.32	0.12891	0.607	1.13

Table 2. TGA and DTG data of $[VO(L^2)(H_2O)] \cdot H_2O$.

Thermo gravimetrical plateau (°C)	DTG (°C)	Mass loss (%)		Process
		Experiment	Calculated	
40–128	48	4.29	5.59	Loss of lattice water
128–321	172	31.43	–	Loss of coordinated water and partial decomposition of the ligand
321–435	365	11.71	–	Partial decomposition of the ligand
435–928	458	44.01	–	Final decomposition of the ligand

Table 3. DTA data of $[VO(L^2)(H_2O)] \cdot H_2O$.

Temperature range (°C)	DTA peaks (°C)	ΔH ($J g^{-1}$)	Process
110–190	139 endo	158.12	Dehydration
414–608	464 exo	1950.20	Decomposition

antiferromagnetically coupled configuration for the Fe(III) and VO(IV) complexes. Such subnormal magnetic moments due to antiferromagnetic interaction in binuclear complexes are well documented [37]. Typical magnetic moment values of 5.83 and 1.79 B.M. are in conformity with high spin mononuclear Fe(III) and VO(IV) complexes. Moderate saturation magnetization and coercivity values of the complexes may qualify the compounds as intermediate magnetic materials.

4.8. *Thermogravimetric analysis*

Thermal investigation of $[VO(L^2)(H_2O)] \cdot H_2O$ was carried out from ambient temperature to 1000°C at a heating rate of 10°C min^{-1}. The decomposition stages have been rationalized (table 2) and corresponding curves are provided in "Supplementary material" (figures 1S and 2S). The DTA data of the complex are presented in table 3. The complex underwent decomposition in four stages. The first (40–128°C) with DTG peak at 48°C corresponds to release of lattice water [38]. The second stage (128–321°C) with DTG peak at 172°C corresponds to loss of coordinated water [39] and partial decomposition of the ligand. The dehydration step is associated with endothermic change in 110–190°C with DTA peak at 139°C. The exothermic change in 414–608°C with DTA peak at 464°C is associated with decomposition of the ligand.

4.9. *Electrochemical behavior*

Electrochemical behaviors of the complexes were studied by cyclic voltammetry at room temperature in 10^{-3} mol L^{-1} dichloromethane solution containing 0.1 mol L^{-1}

Table 4. Electrochemical data of the complexes.

Compound	E_p^a (V)	E_p^c (V)	ΔE (V)	$E_{1/2}$ (V)
$[Fe_2(L^1)_2Cl_2]$	−0.183	−0.738	0.555	−0.460
$[(VO)_2(L^1)_2]\cdot H_2O$	−0.468	−0.525	0.057	−0.496
$[Fe(L^2)Cl]$	−0.311	−0.688	0.377	−0.499
$[VO(L^2)(H_2O)]\cdot H_2O$	−0.357	−0.412	0.055	−0.384

Table 5. Antimicrobial activities of the ligands and their complexes.

	Microorganism (inhibition zone[a] (mm))					
Compound	*K. pneumoniae*	*S. aureus*	*P. aeroginosa*	*E. coli*	*B. subtilis*	*P. vulgaris*
Control	N.O.	N.O.	N.O.	N.O.	N.O.	N.O.
Tetracyclin	16.3 ± 0.6	20.7 ± 0.6	19.0 ± 1.0	22.7 ± 1.2	18.0 ± 0.0	24.7 ± 0.6
H_2L^1	7.7 ± 0.6	10.0 ± 1.0	7.7 ± 1.2	14.0 ± 1.0	12.7 ± 1.2	8.3 ± 0.6
H_2L^2	6.7 ± 0.6	N.O.	N.O.	10.7 ± 1.2	12.0 ± 0.0	N.O.
$[(VO)_2(L^1)_2]\cdot H_2O$	10.0 ± 1.0	13.7 ± 0.6	11.0 ± 0.0	13.0 ± 1.0	10.3 ± 0.6	14.3 ± 1.2
$[VO(L^2)(H_2O)]\cdot H_2O$	N.O.	6.3 ± 0.6	N.O.	N.O.	N.O.	6.3 ± 0.6
$[Fe_2(L^1)_2Cl_2]$	8.3 ± 0.6	12.0 ± 1.0	10.3 ± 0.6	12.3 ± 0.6	11.0 ± 1.0	11.7 ± 0.6
$[Fe(L^2)Cl]$	5.3 ± 0.6	N.O.	N.O.	7.7 ± 1.2	N.O.	N.O.

N.O., not observed.
[a] Including disc diameter 4 mm.

tetrabutyl ammonium perchlorate as supporting electrolyte from −1.2 to 1.2 V *versus* SCE at a scan rate of $100\,\text{mV}\,\text{s}^{-1}$. The electrochemical data are presented in table 4 and corresponding voltammograms are provided in "Supplementary material" (figure 3Sa–Sd). The oxovanadium(IV) complexes exhibit reversible one electron oxidation behavior ($\Delta E \sim 59\,\text{mV}$) assignable to VO(V)/VO(IV) couple [40]. The iron(III) complexes display a quasireversible one electron wave with $\Delta E > 100\,\text{mV}$, assignable to Fe(III)/Fe(II) redox couple. The half-wave potentials ($E_{1/2}$) for the complexes are negative and small, indicating ready redox susceptibility of the compounds. These features render the complexes as valuable catalysts for redox reactions [41]. The free ligands did not show any responses in the potential range of −1.2 to 1.2 V under similar experimental conditions, implying their redox innocent character.

4.10. *Antimicrobial activity*

The ligands and their complexes were assayed for *in vitro* antimicrobial activities against *K. pneumoniae*, *S. aureus*, *P. aeroginosa*, *E. coli*, *B. subtilis,* and *P. vulgaris* at $50\,\mu\text{g}\,\text{mL}^{-1}$ using ethanol as solvent as well as control and tetracyclin as standard drug. The antibacterial activity was evaluated by measuring the zone of inhibition in mm. Ethanol had no inhibitory effect on the bacteria in the concentration studied. The screening data (table 5) revealed that the ligand H_2L^1 and its complexes showed moderate inhibitory activity against all the tested microorganisms. The complexes showed high antibacterial activity against *K. pneumoniae*, *S. aureus*, *P. aeroginosa*,

Table 6. Minimum inhibitory concentrations (MICs) of the ligands and their complexes.

	MIC ($\mu g\,mL^{-1}$)					
Compound	*K. pneumoniae*	*S. aureus*	*P. aeroginosa*	*E. coli*	*B. subtilis*	*P. vulgaris*
H_2L^1	36	39	43	41	36	40
H_2L^2	42	–	–	43	39	–
$[(VO)_2(L^1)_2] \cdot H_2O$	28	34	32	30	32	28
$[VO(L^2)(H_2O)] \cdot H_2O$	–	48	–	–	–	42
$[Fe_2(L^1)_2Cl_2]$	36	38	32	38	30	34
$[Fe(L^2)Cl]$	44	–	–	46	–	–

and *P. vulgaris*. Such an enhancement in the activity of metal complexes against certain specific microorganisms may be explained on the basis of Overtone's concept [42] and Tweedy's chelation theory [43]. The Schiff base H_2L^2 and its complexes were active against some bacterial strains. The minimum inhibitory concentrations (MIC) were determined by broth microdilution method [44]. The observed MIC values in $\mu g\,mL^{-1}$ are reported in table 6, showing minimum inhibitory concentrations between 28–48 $\mu g\,mL^{-1}$. The highest zone of inhibition (14.3 mm) was exhibited by $[(VO)_2(L^1)_2] \cdot H_2O$ against *P. vulgaris*. The least MIC (28 $\mu g\,mL^{-1}$) was also exhibited by the same compound against *K. pneumoniae* and *P. vulgaris*.

5. Conclusion

Complexation of [ONO] donor tridentate Schiff bases with Fe(III) and VO(IV) has been acomplished. Both mono and binuclear complexes have been prepared. Besides, the compounds were characterized by spectral, magnetic, thermal, and electrochemical properties. The magnetic susceptibilities suggest antiferromagnetic interactions between the metal ions in the binuclear complexes. The VO(IV) complexes showed reversible redox behavior while the Fe(III) complexes showed quasireversible redox behavior. *In vitro* antimicrobial activity studies against *K. pneumoniae*, *S. aureus*, *P. aeroginosa*, *E. coli*, *B. subtilis*, and *P. vulgaris* revealed that H_2L^1 derived from 2-aminophenol exhibited maximum inhibitory activity against *E. coli* while its oxovanadium complex showed promising inhibitory effect against *P. vulgaris*. The synthetic strategy may serve as a paradigm for accessing new mononuclear and binuclear Schiff-base complexes. The pendent phenolic-OH group on the amine of the dibasic tridentate ligand, L^1, bridges two Fe(III) centers to form $[Fe_2O_2]$ dinuclear core with a chloride on each Fe(III) compensating the overall charge. $VOSO_4 \cdot 5H_2O$ readily forms the spontaneously charge-balanced $[(VO)_2O_2]$ core. For L^2, the carboxylato group on the amine is stereochemically not poised for bridging structures leading to mononuclear complexes with aquo or chloro as ancillary ligands. The complexes were all obtained as coordinatively unsaturated species. The possibilities of solvent molecules coordinating the vacant sites were ruled out from elemental analysis and FT-IR spectroscopy. The complexes reported herein may be used as catalysts in various redox reactions.

Acknowledgments

The authors express sincere thanks to SAIF, NEHU, Shillong; SAIF, CDRI, Lucknow; SAIF, STIC, Kochi, and CIF, IIT, Guwahati, India, for providing analytical and spectral results.

References

[1] K.B. Gudasi, S.A. Patil, R.S. Vadari, R.B. Shenoy, M.S. Patil. *Transition Met. Chem.*, **30**, 1014 (2005).
[2] A.P. Ginsberg, E. Koubek, H.J. Williams. *Inorg. Chem.*, **5**, 1656 (1966).
[3] K.C. Dash. *J. Ind. Chem. Soc.*, **72**, 359 (1995).
[4] J.B. Vincent, T. Hui-Lún, A.B. Blackman, E.B. Lobkovsky, D.N. Hendrickson, G. Christoug. *J. Am. Chem. Soc.*, **115**, 2353 (1993).
[5] C. Kaes, A. Katz, M.W. Hosseini. *Chem. Rev.*, **100**, 3533 (2000).
[6] G. Psomas, C. Dendrinou-Samara, P. Philippakopoulos, V. Tangoulis, C.P. Raptopoulou, E. Samaras, D.P. Kessissoglou. *Inorg. Chim. Acta*, **272**, 24 (1998).
[7] P. Losier, M.J. Zaworotka. *Angew. Chem. Int. Ed. Engl.*, **35**, 2779 (1996).
[8] R. Kruszynski, B. Kuznik, T.J. Bartczak, D. Czakis-Sulikowska. *J. Coord. Chem.*, **58**, 165 (2005).
[9] J.M. Li, Y.G. Zhang, J.H. Chen, L. Rui, Q.M. Wang, X.T. Wu. *Polyhedron*, **19**, 1117 (2000).
[10] J.H. Liao, S.H. Cheng, C.T. Su. *Inorg. Chem. Commun.*, **5**, 761 (2002).
[11] H.L. Singh, M. Sharma, A.K. Varshney. *Synth. React. Inorg. Met. Org. Chem.*, **30**, 445 (2000).
[12] M. Kohutova, K. Valent, E. Misikova, D. Mlynarcik. *Chem. Pap.*, **54**, 87 (2000).
[13] M. Nath, S. Pokharia, R. Yadav. *Coord. Chem. Rev.*, **215**, 99 (2001).
[14] P.G. Cozzi. *Chem. Soc. Rev.*, **33**, 410 (2004).
[15] S.K. Edulji, S.T. Nguyen. *Organometallics*, **22**, 3374 (2009).
[16] J.A. Miller, W. Jin, S.T. Nguyen. *Angew. Chem. Int. Ed.*, **41**, 2953 (2002).
[17] G.A. Kolawole, A.A. Osowok. *J. Coord. Chem.*, **62**, 1437 (2009).
[18] M.R. Maurya. *Coord. Chem. Rev.*, **237**, 163 (2003).
[19] D. Rehder. *Coord. Chem. Rev.*, **182**, 297 (2003).
[20] A. Butler, M.J. Clague, G.E. Meister. *Chem. Rev.*, **94**, 625 (1994).
[21] C.J. Carrano, C.M. Nunn, R. Quan, J.A. Bonadies, V.L. Pecoraro. *Inorg. Chem.*, **29**, 944 (1990).
[22] G. Asgedom, A. Sreedhara, J. Kivikoski, C.P. Rao. *Polyhedron*, **16**, 643 (1997).
[23] N.R. Sangeetha, V. Kavita, S. Wacadlo, A.K. Powell, S. Pal. *J. Coord. Chem.*, **59**, 55 (2000).
[24] C.R. Bhattachaejee, P. Goswami, P. Mondal. *J. Coord. Chem.*, **63**, 2002 (2010).
[25] G.A. Barclay, C.M. Harris, B.T. Hoskins, E. Kokot. *Proc. Chem. Soc.*, 264 (1961).
[26] V.B. Badwaik, R.D. Deshmuk, A.S. Aswar. *J. Coord. Chem.*, **62**, 2037 (2009).
[27] J. Han, Y.H. Xing, F.Y. Bai, X.J. Zhang, X.Q. Zeng, M.F. Ge. *J. Coord. Chem.*, **62**, 2719 (2009).
[28] B. Chiswell, J.P. Crawford, E.J. O'Reilly. *Inorg. Chim. Acta*, **49**, 223 (1980).
[29] N. Nawar, N.M. Hosny. *Transition Met. Chem.*, **25**, 1 (2000).
[30] M. Tumer, H. Koksal, S. Serin. *Synth. React. Inorg. Met. Org. Chem.*, **27**, 775 (1997).
[31] K. Nakamoto. *Infrared and Raman Spectra of Inorganic and Coordination Compounds*, 4th Edn, John Wiley and Sons, Inc., New York (1986).
[32] S.N. Rao, K.N. Munshi, N.N. Rao, M.M. Bhadbhade, E. Suresh. *Polyhedron*, **18**, 2491 (1999).
[33] M.R. Maurya, A. Kumar. *J. Mol. Catal. A: Chem.*, **250**, 190 (2006).
[34] M.R. Maurya, S. Khurana, C. Schulzke, D. Rehder. *Eur. J. Inorg. Chem.*, **3**, 779 (2001).
[35] A.B.P. Lever. *Inorganic Electronic Spectroscopy*, 2nd Edn, Elsevier, Amsterdam (1984).
[36] W.J. Geary. *Coord. Chem. Rev.*, **7**, 81 (1971).
[37] M.R. Truter. *Chem. Brit.*, **7**, 203 (1971).
[38] S.A. Sallam. *Transition Met. Chem.*, **31**, 46 (2006).
[39] K.H. Mostaga, M.H. Repat, A.A. Mohamed. *Monatsch. Chem.*, **122**, 829 (1991).
[40] A.A. Nejo, G.A. Kolawole, A.R. Opoku, C. Muller, J. Wolowska. *J. Coord. Chem.*, **62**, 3411 (2009).
[41] F.R. Perez, L. Basaez, J. Belmar, P. Vanysek. *J. Chil. Chem. Soc.*, **50**, 575 (2005).
[42] N. Dharamaraj, P. Viswanathamurthi, K. Natarajan. *Transition Met. Chem.*, **26**, 105 (2001).
[43] R. Malhota, S. Kumar, K.S. Dhindsa. *Indian J. Chem.*, **32A**, 457 (1993).
[44] J.H. Jorgensen, J.D. Turnidge. *Manual of Clinical Microbiology*, 8th Edn, American Society for Microbiology, Washington, DC (2003).